NEODYMIUM LASER GLASS
IMPROVEMENT PROGRAM

Technical Summary Report

Number 10

March 1971

AMERICAN OPTICAL
CORPORATION

CENTRAL RESEARCH LABORATORY · SOUTHBRIDGE, MASS. 01550

DDC

TR 598-10

This research is part of Project DEFENDER under the
joint sponsorship of the Advanced Research Projects
Agency, the Office of Naval Research and the
Department of Defense.

Reproduction in whole or in part is permitted by the
United States Government.

Distribution of this document is unlimited.

NEODYMIUM LASER GLASS
IMPROVEMENT PROGRAM

Technical Summary Report

Number 10

March 1971

Dr. Richard F. Woodcock

Contract No. Nonr-3835(00)
Project Code No. 7300
ARPA Order No. 306

American Optical Corporation
Central Research Laboratory
Southbridge, Mass. 01550

D D C
RECEIVED
4 1971
B

DOCUMENT CONTROL DATA - R & D

(Security classification of title, body of abstract and indexing annotation must be entered when the overall report is classified)

1. ORIGINATING ACTIVITY (Corporate author)	2a. REPORT SECURITY CLASSIFICATION
American Optical Corporation Central Research Laboratory Southbridge, MA. 01550	Unclassified
	2b. GROUP N/A

3. REPORT TITLE

NEODYMIUM LASER GLASS IMPROVEMENT PROGRAM

4. DESCRIPTIVE NOTES (Type of report and inclusive dates)

Technical Summary Report   1 January 1967 - 30 June 1967

5. AUTHOR(S) (First name, middle initial, last name)

Richard F. Woodcock

6. REPORT DATE March 1971	7a. TOTAL NO. OF PAGES 36	7b. NO. OF REFS 3
8a. CONTRACT OR GRANT NO. Nonr 3835(00) b. PROJECT NO. 7300 c. ARPA ORDER 306 d.	9a. ORIGINATOR'S REPORT NUMBER(S) TR-598-10	
	9b. OTHER REPORT NO(S) (Any other numbers that may be assigned this report)	

10. DISTRIBUTION STATEMENT

Distribution of this report is unlimited

11. SUPPLEMENTARY NOTES Project DEFENDER	12. SPONSORING MILITARY ACTIVITY Office of Naval Research Washington, D.C.

13. ABSTRACT

This report details efforts expended toward achieving a means for measuring the stress optical coefficients of both homogeneous and inhomogeneous laser glass test specimens. The design of a 3-pinhole interferometer is discussed and tests made are presented. Elastic properties are briefly treated as is information on glass sample preparation. Finally, a theoretical analysis of the three pinhole interferometer is appended.

14. KEY WORDS	LINK A		LINK B		LINK C	
	ROLE	WT	ROLE	WT	ROLE	WT
Lasers						
Laser Glass						
Interferometer						

FOREWORD

This report has been prepared by the Central Research Laboratory of the American Optical Corporation, Southbridge, Massachusetts under Contract Nonr 3835(00) entitled "Neodymium Laser Glass Improvement Program." The contract is under the sponsorship of the Office of Naval Research and this report covers the six-month period ending 30 June 1967.

Dr. Richard F. Woodcock is project manager. Luther Smith was involved in the design, analysis and operation of the pinhole interferometer described herein. Theoretical considerations included as Appendix I were carried out by Dr. H. Osterberg and L. Smith.

This program is part of project DEFENDER.

This report is unclassified.

CONTENTS

BLANK PAGE

NEODYMIUM LASER GLASS IMPROVEMENT PROGRAM

1. INTRODUCTION AND SUMMARY

This technical summary covers work performed under contract Nonr 3835 (00) during the six month period ending 30 June 1967. Efforts during this period have been concerned primarily with the design of an improved system for measuring stress optical coefficients.

Previous experimental work on the measurement of stress optical coefficients of both homogeneous and inhomogeneous test specimens indicate that a better method of measurement is required in the latter case. To obtain stress optical coefficients with a precision of 5-10% requires a sensitivity in the interferometric measurements of 1/100 wavelength. This accuracy requirement, together with the fact that the test specimens will undoubtedly contain some degree of inhomogeneity, has led to the choice of a Zernike type interferometer for this measurement.

Theoretical analysis and experimental evaluation of the tolerances required in this instrument and related components are in progress prior to finalizing the detailed design of the apparatus. The effect of the following factors on the linearity of the interferometer measurement and its stability were investigated during this period; (1) The need for locating the three pin holes in the front focal plane of the telescope lens, (2) equality of spacing of the pin holes, (3) slight defocusing of the collimator, (4) tilt of the test specimen, and (5) motion of the pin holes with respect to the test specimen and the measuring apparatus.

The interferometer will measure the change in optical thickness which is due to the combined effects of the change in refractive index and the change in sample dimensions as a function of applied stress. Since the stress optical coefficients are related only to the index changes, factors containing the change in sample dimensions [cf. Appendix I] must be subtracted from the observed change in pathlength. Dimensional changes of the specimen will be calculated from measured values of the applied pressure (P), Young's Modulus (E) and Poisson's Ratio (σ). The elasticity constants will be determined from an

1

independent measurement of the velocity of sound on samples taken from the same glass melt as the stress optic coefficient samples. Preparation of glass of suitable quality and of the test specimens for the above measurements have proceeded during this period.

2. STRESS OPTICAL COEFFICIENT MEASUREMENT

It is well known that a block of glass acted upon by non-uniform pressure resulting from a thrust or tension normally becomes doubly refracting, behaving as a uniaxial, optically negative crystal with the optic axis parallel to the local direction of the stress, and with a birefringence proportional to the intensity of the stress. This phenomenon is analyzed theoretically[1] [also appendix] in terms of two stress-optical coefficients (p/ν) and (q/ν) that are related to the stress-induced changes in pathlength for linearly polarized light passing through the glass block. The experimental measurement of these changes in pathlength for optically inhomogeneous blocks of glass from 7 to 10 mm in thickness has been undertaken at this time. The experience of previous investigators[2] indicate that an interferometric method with a sensitivity of 1/100 wavelength of phase change will be necessary in order to determine the stress-optical coefficients with a precision of 5 to 10%.

2.1 INTERFEROMETER DESIGN

Whereas many interferometers can be used to measure the changes in optical pathlength for homogeneous samples of high quality, most of them are eliminated when glass containing striae is to be measured with precision. Thus, the Jamin interferometer used by Pockels, and indeed any wavefront shearing interferometer cannot be used because of the irregular fringes that appear with optically inhomogeneous samples. One way out of this difficulty is to arrange to measure the average optical path through a small area of the specimen, which suggests the use of a pinhole interferometer. The three-pinhole method due to Zernike[3] operates in this fashion and produces fringe patterns with excellent regularity of spacing even when the glass specimen is quite non-uniform optically. The method also appears to have the necessary sensitivity and is, therefore, the method chosen for modification to make the present measurements.

Figure 1 is a plan view of the basic three-pinhole interferometer. The glass sample is strained by compression along an axis perpendicular to the plane of the figure, while the light passing through the system is linearly polarized. The cross section of the glass samples is nominally 10 mm x 10 mm, so the pinholes are separated by some 7 mm center-to-center. Because the radiation coming through them must interfere at and near the back focal plane of the telescope lens they must be illuminated by light with good spatial and temporal coherence. The need for coherence, the need for polarized light and the need for sufficient intensity to make visual observations on the interference fringes have led to the use of a He-Ne cw laser (0.1 milliwatt single mode output) to illuminate the collimator pinhole O.
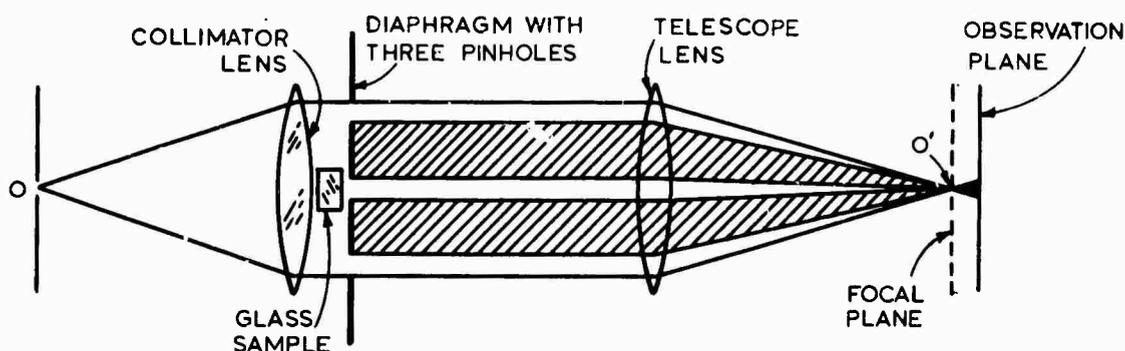
Figure 1. The basic three pinhole interferometer. Light from a laser is focused upon the pinhole O. The interference pattern in the observation plane is examined through a microscope (~100x mag.).

It can be shown [c.f. appendix] that if the three pinholes are of equal size, are equally spaced in a straight line, are small compared to their separation and are placed in the front focal plane of the telescope lens, then the interference pattern in a small neighborhood of the back focal point of the lens is periodic along the optic axis as well as along a direction parallel to the line joining the centers of the pinholes. If the coherent light beams from the three pinholes are all in phase, the back focal plane itself will contain a set of fringes that are equally spaced and alternate in intensity, with

the strong fringes 9 times as intense as the weak ones. This pattern is repeated in planes parallel to the back focal plane and spaced at equal intervals from it both inside and outside of focus. However, in adjacent planes, the strong fringes have exchanged places with the weak fringes. See Figure 2. Half way between these planes are planes in which the fringes are equally spaced and all of the same intensity. The eye is very good at judging the intensity match between adjacent fringes, so it is one of these latter planes that is followed during measurements because it is so accurately identifiable visually.
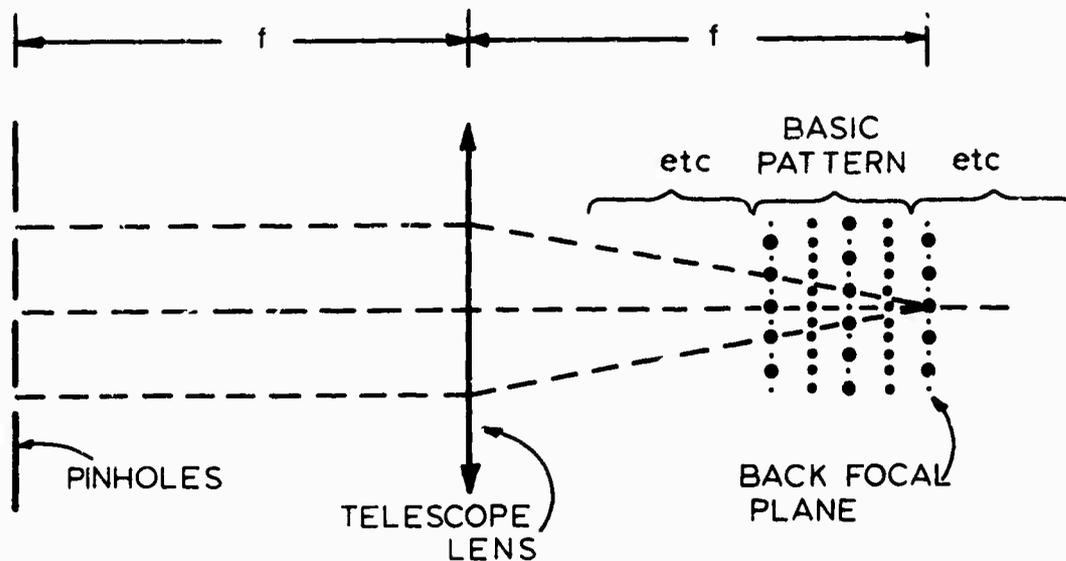
Figure 2. Illustration of the fringe system near focus in the Zernike interfercmeter. The fringes extend in and out of the plane of the figure. Their relative intensities are indicated by the size of the dots. Fringe spacing is not to scale.

The entire family of fringes will shift in or out along the optic axis as the phase of the beam from the central pinhole is changed relative to that for the two side pinholes. Furthermore, the amount of shift is directly proportional to the amount of phase shift, so if a microscope is arranged to focus on one of the fringe patterns and can be moved in and out along the optic axis in a controlled and measurable way, a phase shift in the central beam can be translated into motion of the microscope and can be measured thereby. The constant of proportionality is obtained by considering the geometry of the three converging beams. For example, to maintain a chosen phase relation between the light from the three beams arriving at an axial point as the phase of the central beam is retarded more and more, the point must be moved in along the axis since such a motion shortens the geometrical path from the central hole to the point more than it shortens the paths from the side holes to the point.

This geometrical effect also exists in the three-dimensional stationary fringe pattern of the undisturbed beams; the distance the microscope must be moved to focus first on one plane where the fringes are <u>all</u> <u>of</u> <u>equal</u> <u>intensity</u> and then on an adjacent plane containing an identical pattern corresponds to a <u>one-half</u> wavelength phase change in the light from the central hole relative to that from the side holes. The interferometer is "self calibrating" in this manner and the size and spacing of the pinholes need not be known at all while the focal length of the telescope lens need be known only approximately.

2.2 TEST OF DESIGN

Preliminary tests of various components of the system have been carried out to establish the validity of the overall design of the system and to establish the tolerances required in specific components. In these tests stress was applied to the sample with the arbor press and sample fixtures used in the original stress optical coefficient measurement studies while an improved design of these components, dictated by the results of the original study is being formulated.

5

2.2.1 Fringe Formation and Stability

It has been established that illumination of suffi-
cient intensity, coherence and degree of polarization to produce
clear interference fringes in this system can be obtained by
passing light from a Spectra-Physics Mod. 130 He-Ne laser through
a 20x microscope objective to focus it down on an 8 μm diameter
pinhole (pinhole O in Fig. 1) after which it diverges to a 38 cm
focal length doublet serving as collimator lens. Various com-
binations of the three pinholes that mask out all but three
small pencils of light in the collimated beam illuminating the
sample have been tried. Consistent with the theory, the use of
a central pinhole of larger diameter than the two outer holes
is not necessary. In our application it is preferable to let
the three pinholes have the same diameter. Also, it is prefer-
able to keep the central pinhole as small as practically possible
in order to obtain the measurement of the average optical path
over the selected area of a glass sample with striae. Three
pinholes having the diameter of about 0.34 mm and separated by
7 mm provide enough light in the fringes. The use of even
smaller pinholes may be possible, but pinholes having diameters
of 0.50 mm or more produce a fringe system that has too small
lateral extent in this application.

In these early experiments it was found that good
fringe settings could be obtained whether the central pinhole
was uncovered or covered with uniform or nonuniform blocks of
glass. The fringe settings with glass in the central pencil of
light, however, drifted rapidly with time whenever the tem-
perature of the sample was changing. It will be necessary to
smooth out the effect of the 2 to $3^{\circ}C$ temperature fluctuations
within the air-conditioned measurement laboratory by surrounding
the sample, and perhaps the entire interferometer, with a
secondary iso-thermal enclosure.

2.2.2 Interferometer Calibration vs Pinhole Location

With respect to the scheme of Fig. 1, the collimator
and telescope lenses are of about 38 cm focal length. Observa-
tion planes near the focal plane O^1 are observed with a micro-
scope having a 10x objective and a 10x eyepiece with reticle so
that one can concentrate on a particular localized region of the
fringe pattern when necessary. The microscope body tube is

mounted on a small, sliding table actuated by a thimble micro-
meter so that the microscope can be moved along the optic axis
of the interferometer in a controlled manner and the displace-
ment be read to ± 0.00254 mm. A total motion of 2.54 cm is
possible.

With the interferometer in adjustment, a sequence of
10 readings from the micrometer of repeated settings when the
observer judges that the magnified fringes seen in the micro-
scope are all of the same intensity will have a standard devia-
tion .01270 to .01524 mm. The distance between planes in which
the fringes are all of the same intensity is about 1.854 mm
for our choice of pinhole spacing and focal length of the tele-
scope lens. As explained in Sect. 2.1 this distance represents
a pathlength change of 1/2 wavelength between the light coming
from the center pinhole and that coming from the two outer pin-
holes in the interferometer, hence we have the sensitivity to
detect changes as small as $0.0127 \div 3.7 \approx 0.0034$ wavelength.
If the interferometer can be made with sufficient stability the
goal of measuring pathlength changes to 0.02 wavelength will
certainly be met.

The displacement δz (approx. 1.854 mm in our case)
that alters the phase by π (a pathlength change of 1/2 wave-
length) is predicted by theory to be a constant no matter which
two adjacent planes of equal-intensity fringes are examined near
the back focal plane of the telescope lens provided the triplet
of pinholes is located at the front focal plane. This has been
found to be the case for a range of 6 1/2 wavelengths of path
change both inside and outside the back focus, a range that
exceeds by a healthy margin the pathlength changes expected
from straining the glass samples. It will be safe, therefore,
to determine this "calibration" distance over one part of this
range and apply it to phase change measurements in another part.

When the triplet of pinholes was positioned several
centimeters nearer the telescope lens, the "calibration" dis-
tance δz became a function of the distance from the back focal
plane at which the fringes were examined. The change was per-
ceptible, but the tolerance on positioning the triplet of pin-
holes is judged to be ± 2.54 mm. That is, translations of
$\mp$ 2.54 mm along the axis of the interferometer from the
first focal plane of the telescope are not large enough to
matter.

7

2.2.3 Tolerance of Pinhole Spacing

The effect of unequal spacing of the pinholes, i.e.
inaccurate positioning of the central pinhole between the two
outer pinholes was studied theoretically. The conclusion is
that the central hole must not be located off-center by any more
than 0.0254 mm, a tolerance that can be met with relative ease.

2.2.4 Tolerance on Sample Alignment

The most damaging effect of the tilt of the sample
from perpendicularity to the incident collimated light is the
change in tilt that may be produced upon changing the pressure
applied to the sample. That is, a slight rotation of the sample,
bodily, will introduce a change not related to the stress-optical
effect in the pathlength for light passing through the sample
and the central pinhole. The effect of change in tilt depends
on the initial amount of tilt, being a minimum when the nominally
parallel faces of the sample are perpendicular to the incident
light. Some simple geometrical optical calculations show that,
for example, if the sample has an initial tilt of $0.1°$ then an
additive change in tilt (assuming 10 mm of glass with a refrac-
tive index of 1.5) of $0.05° = 3$ min. will cause an error of 0.01
wavelength in the measurement of change in pathlength.

Accordingly, the head of an autocollimating device
will be placed just beyond the pinhole O, Fig. 1 for the purpose
of monitoring how nearly normal the surfaces of the glass sample
are to the incident beam. During initial sample alignment
motion of the return beam in two directions should be watched
and the resultant not allowed to exceed about 7 minutes of arc.
he change in tilt during the application of stress to the sample
should not exceed about 20 seconds of arc.

2.2.5 Tolerance on Lateral Pinhole Motion

During the measurement one can hardly expect to
tolerate any relative motion between the glass sample and the
central pinhole when the glass has striae or other inhomogeneities.
A rough experimental check on this point using a glass block
with striae visible to the unaided eye showed that relative
motion as large as 2.5 μm caused interferometric phase changes
easily visible in the fringe pattern of the interferometer.

8

It is necessary, then, to attach the triplet of pinholes to the glass sample (in a manner that will not interfere with the strain pattern) so that relative motion between the two is virtually eliminated. When this is done, the sample-plus-pin-holes can be translated by as much as 0.25 mm with no detectable effect on the fringe pattern.

2.2.6 The strain-frame

As a result of the tests and checks made during this period and the response to inquiries to manufacturers of laboratory presses, it has been decided that a weight-and-fulcrum device will be constructed to provide constant vibration-free straining of the glass samples. The frame will be designed so that the sample can be aligned to have its polished faces accurately perpendicular to the incoming beam of light from the interferometer collimator head and will be sturdy enough so that the sample will not move appreciably as the load is applied. It will have a low profile so that it and the interferometer can all be covered with a secondary thermal shield built to cover the granite test block (1.2 × 2.4 m) which will serve as a base.

3. ELASTIC PROPERTIES

As stated in Section 1 the change in optical thickness of a test specimen as a function of applied pressure is a combination of a change in refractive index and a change in physical dimensions. The stress optical coefficient relates only to the change in index and, therefore, the change in pathlength due to the change in sample dimension must be accounted for. The change in sample thickness can either be measured directly or calculated. The latter was chosen because of better accuracy. The change in sample thickness per unit length, $\Delta L/L$, along the optical axis of the interferometer, i.e. normal to the direction of applied pressure, is given by the following expression;

$$\frac{\Delta L}{L} = \frac{\sigma P}{E} \quad ,$$

where P is the measured value of applied pressure, E is Young's Modulus and σ is Poisson's Ratio.

9

Values of Young's Modulus and Poisson's Ratio will be calculated from measurements of the acoustical velocities in the glass of both longitudinal waves, V_L, and shearwaves, V_s. The relationship between these wave velocities and the values of Young's Modulus and Poisson's Ratio are given by the following;

$$C_1 = V_L^2 \rho = \lambda + 2\mu$$

$$C_s = V_s^2 \rho = \mu$$

and

$$E = \frac{\mu(2\mu + 3\lambda)}{\lambda + \mu}$$

$$\sigma = \frac{\lambda}{2(\lambda + \mu)} \quad .$$

Apparatus for the measurement of the acoustic velocity of longitudinal and shearwaves on a fairly routine basis exists at MIT. Measurement on samples $1.65 \times 1.65 \times 1.27$ cm will be made on that equipment under the guidance of Professor S. C. Moss. To date, samples of seven glass compositions have been supplied for this measurement.

4. GLASS PREPARATION

Previous results indicated that considerable improvement could be made in the optical quality of experimental glasses to be used in the measurements of stress optical coefficients, by making a slightly larger melt with special care taken to achieve the correct melting and stirring cycles. The results obtained on 0.9 kg melts have continued to be encouraging. About 15 melts of the 0.9 kg size or larger have been received to date which contained portions of sufficiently good optical quality to satisfy our present needs. The remaining athermal compositions will be melted in a similar manner where necessary.

As these melts are completed the top and bottom surfaces are polished and the areas of acceptable optical quality are

10

mapped out. Test specimens 1 × 1 × 3 cm, for the measurement of the change in pathlength as a function of pressure, and 1.65 × 1.65 × 1.27 cm, for the determination of Young' Modulus and Poisson's Ratio, are then prepared from these areas of good optical quality. This work will continue so that test specimens and auxillary data will be available for the determination of stress optical coefficients when the apparatus for measuring the change in optical pathlength is completed.

REFERENCES

1. "Properties of Glass," by G. W. Morey, Reinhold Pub. Corp. New York, 1954, 2nd Ed., pp. 442-451. See also L. H. Adams and E. D. Williamson, J. Wash. Acad. 9, 609-623 (1919).

2. F. Pockels, Annalen der Physik (ser. 4) 7, 745-771 (1902), (ser. 4) 9, 220-223 (1902) and (ser. 4) 11, 651-653 (1903).

3. F. Zernike, J. Opt. Soc. Amer. 40, 326-328 (1950). See also: B. Vittoz, Helv. phys. Acta 26, 400-403 (1953) and A.C.S, vanHeel, Physica XXIV, 529-531 (1958).

APPENDIX I

THEORETICAL CONSIDERATIONS OF ZERNIKE'S THREE PINHOLE INTERFEROMETER AS APPLIED TO THE MEASUREMENT OF STRESS OPTICAL COEFFICIENTS IN STRIATED GLASSES

I.1 INTRODUCTION

The effect of pressure on the optical properties of glass is described by Morey, "Properties of Glass," Reinhold Publishing Corporation, 1954, 2nd Ed. pp 442-451. We adhere to the theory given by Morey. The pressure P is applied along Z and the light is propagated along Y as in Fig. I-1. The electric vector is polarized to vibrate along Z or X.
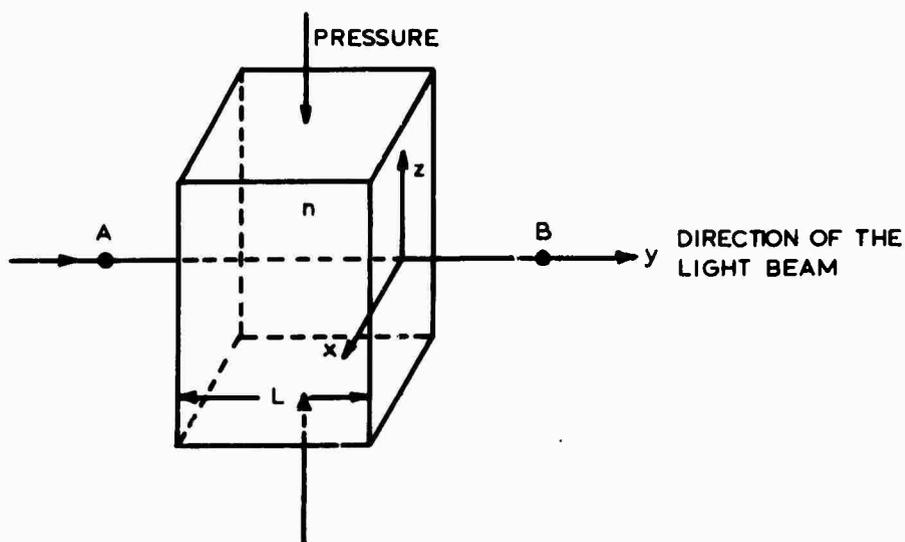
Figure I-1. Convention with respect to the glass sample. n is the refractive index of the isotropic solid when no stress is applied.

13

Let X_x, Y_y and Z_z be the longitudinal components of strain. Let ν be the velocity of light in the glass in the unstrained state. Let ν_x, ν_y and ν_z denote the velocities with the electric vector vibrating along X, Y and Z respectively. Then, beginning from the relations

$$\nu_x - \nu = q\, X_x + p\, Y_y + p\, Z_z \ ;$$

$$\nu_y - \nu = p\, X_x + q\, Y_y + p\, Z_z \ ;$$

$$\nu_z - \nu = p\, X_x + p\, Y_y + q\, Z_z \ ; \tag{1}$$

and introducing

$$X_x = Y_y = \sigma \frac{P}{E} \ ; \qquad Z_z = -\frac{P}{E} \ ; \tag{2}$$

P = pressure; E = Young's modulus; σ = Poisson's ratio; then since

$$\frac{\nu_x - \nu}{\nu} = \frac{n - n_x}{n_x} \ ; \qquad \frac{\nu_y - \nu}{\nu} = \frac{n - n_y}{n_y} \ ; \qquad \frac{\nu_z - \nu}{\nu} = \frac{n - n_z}{n_z} \ ; \tag{3}$$

we obtain witn respect to Fig. I-1.

$$\frac{n_z - n}{n_z} \equiv \frac{\Delta n_z}{n_z} \rightarrow \frac{\Delta n_z}{n} = \frac{P}{E}\left[\frac{q}{\nu} - 2\sigma\frac{p}{\nu}\right] \ ; \quad \text{(Z-polarization)}$$

$$\frac{n_x - n}{n_x} \equiv \frac{\Delta n_x}{n_x} \rightarrow \frac{\Delta n_x}{n} = \frac{P}{E}\left[(1-\sigma)\frac{p}{\nu} - \sigma\frac{q}{\nu}\right] \cdot \quad \text{(X-polarization)} \tag{4}$$

14

In summary

$$\frac{\Delta n_z}{n} = \frac{P}{E}\left[\frac{q}{\nu} - 2\sigma\frac{p}{\nu}\right];\ \text{Z-polarization:}$$

$$\frac{\Delta n_x}{n} = \frac{P}{E}\left[(1-\sigma)\frac{p}{\nu} - \sigma\frac{q}{\nu}\right];\ \text{X-polarization:} \tag{5}$$

Z along line of pressure X ⊥ line of pressure.

The problem is to measure $\Delta n_z/n$ and $\Delta n_x/n$ so that the coefficients p/ν and q/ν can be computed from Eq. 5.

I.1.1 General Scheme for Measuring $\Delta n_x/n$ and $\Delta n_z/n$.

With reference to Fig. I-1, let D be the distance in air from A to B. Let ϕ denote optical path in number of wavelengths.

$$\phi = \phi_0 \text{ for no pressure; } \phi = \phi_a \text{ with pressure applied.} \tag{6}$$

$$\phi_0 = \frac{L(n-1) + D}{\lambda}\ ; \ \phi_a = \frac{(n+\Delta n-1)(L+\Delta L)+D}{\lambda}\ . \tag{7}$$

Then

$$\Delta\phi \equiv \phi_a - \phi_0 = \frac{L\Delta n+(n-1)\Delta L}{\lambda}\ ;\ \Delta n\Delta L \text{ neglected.} \tag{8}$$

$$\therefore\ \frac{\Delta n}{n} = \frac{\lambda\Delta\phi}{nL} - \frac{\Delta L}{L}\frac{n-1}{n}\ \text{ or, again,}$$

$$\left.\frac{\Delta n}{n} = \frac{\lambda\Delta\phi}{nL} - \sigma\frac{P}{E}\frac{n-1}{n}\ ;\ \frac{\Delta L}{L} = \frac{\sigma P}{E}\ \right\}. \tag{9}$$

15

Either one measures both $\Delta\phi$ and ΔL or measures $\Delta\phi$ and P while knowing σ and E. At the moment we do not plan to measure ΔL.

Let

$$\Delta\phi_x = \Delta\phi \text{ for the E-vector along X;}$$

$$\Delta\phi_z = \Delta\phi \text{ for the E-vector along Z, the line of pressure.}$$

Then

$$\frac{\Delta n_x}{n} = \frac{\lambda\Delta\phi_x}{nL} - \frac{\sigma P}{E}\frac{n-1}{n} \; ; \; \frac{\Delta n_z}{n} = \frac{\lambda\Delta\phi_z}{nL} - \frac{\sigma P}{E}\frac{n-1}{n} \; ;$$

$$\Delta n_x \equiv n_x - n; \; \Delta n_z = n_z - n. \tag{10}$$

We thus have a definite way of obtaining $\Delta n_x/n$ and $\Delta n_z/n$ if we arrange to measure the changes of optical path $\Delta\phi_x$ and $\Delta\phi_z$.

I.2 CHECK ON THE VALUE OF $\Delta\phi_z$ AGAINST POCKELS,
     [Annalen der Physik (Ser. 4) 7:745-771 (1902).] From
     Eq. (10)

$$\frac{\lambda\Delta\phi_z}{nL} = \frac{\Delta n_z}{n} + \frac{\sigma P}{E}\frac{n-1}{n} \tag{11}$$

Then from Eqs. (11) and (5)

$$\Delta\phi_z = \frac{nL}{\lambda}\frac{P}{E}\left[\sigma\frac{n-1}{n} + \frac{q}{\nu} - 2\sigma\frac{p}{\nu}\right]; \tag{12}$$

which agrees with Eq. (2) on p. 748 of Pockel's paper.

16

Let us look also into the value of $\Delta\phi_x$. From Eq. (10)

$$\frac{\lambda\Delta\phi_x}{nL} = \frac{\Delta n_x}{n} + \sigma\frac{P}{E}\frac{n-1}{n} \tag{13}$$

Then from Eqs. (13) and (5)

$$\Delta\phi_x = \frac{nL}{\lambda}\frac{P}{E}\left[\sigma\frac{n-1}{n} + (1-\sigma)\frac{P}{\nu} - \sigma\frac{q}{\nu}\right]. \tag{14}$$

Now, interestingly, we see that from Eqs. (12) and (14) that

$$\Delta\phi_x - \Delta\phi_z = \frac{nL}{\lambda}\frac{P}{E}(1+\sigma)\left[\frac{P}{\nu} - \frac{q}{\nu}\right]. \tag{15}$$

It can happen that for flint glasses q > p; but from Pockel's data p is usually greater than q. Thus we must expect that, usually,

$$\Delta\phi_x > \Delta\phi_z. \tag{16}$$

I.3 COMMENTS ON STRIATED GLASS

Whereas many interferometers can be used to measure the optical path differences $\Delta\phi_x$ and $\Delta\phi_z$ for homogeneous glass of high quality, most of the methods must be eliminated when striated glasses are to be measured with a high degree of precision. We would like to measure $\Delta\phi_x$ and $\Delta\phi_z$ to about $\lambda/100$ - even though the glass be quite striated. Thus, the method of the Jamin interferometer, as used by Pockels with great success, fails. Other interferometers, such as the Tyman-Green, fail also because the optical paths of the two arms are too unstable thermally. In so far as possible, the two interfering beams should follow practically parallel paths, and the interferometer, should produce straight fringes even though the glass is quite nonuniform.

17

Let the beam passing through the glass sample be called the object beam. If the glass is striated, one way out of the difficulty is to arrange to measure the **average** optical path through a **small** area of the sample. This suggests the use of the double pinhole interferometer: but further considerations lead one to the choice of the three pinhole method due to Zernike. Certain modifications become desirable.

I.4 A ZERNIKE PINHOLE SYSTEM; THE AVERAGING EFFECT OVER A CENTRAL, SMALL PINHOLE

We prefer to begin by considering the configuration of Figure I-2 in which the lenses are omitted.
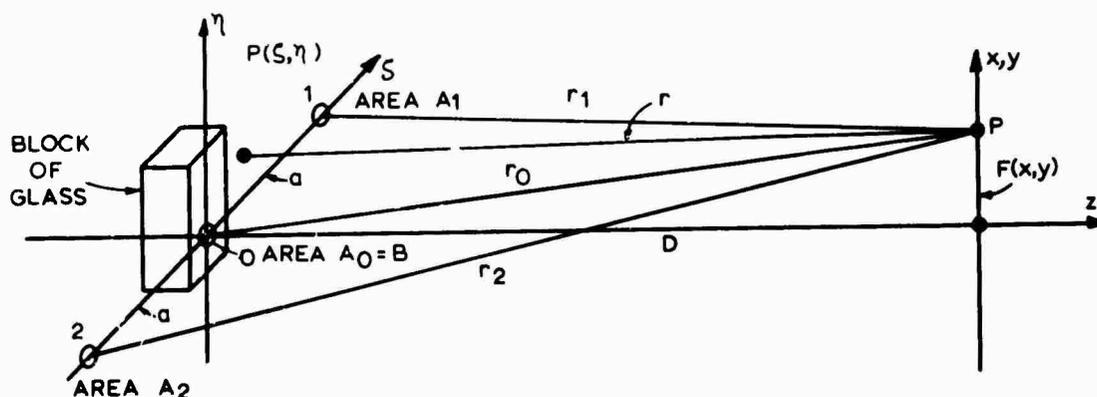
Figure I-2. Pinholes are located at $\zeta = \pm$ a, η = o and at ζ = o, η = o. A block of glass is placed behind pinhole #o, the central pinhole. The areas of the pinholes are A_1, A_2 and B, as indicated. We suppose for convenience that incident upon the plane of the pinholes is a plane wave propagated along Z. Pinholes #1 and 2 are clear.

If P(ζ, η) is the complex transmittance at the "object plane" ζ, η, then from Huygens' principle the disturbance F(x, y) = F(x, y, D) is given by

$$F(x,y) = \iint_{\text{over } \zeta, \eta - \text{plane}} P(\zeta, \eta) \frac{e^{ikr}}{r} d\zeta d\eta \; ; \tag{17}$$

$$r = \sqrt{(\zeta-x)^2 + (\eta-y)^2 + D^2}$$

We are not at liberty to assert that the plane Z=D falls in the Fraunhofer region so that $F(x,y)$ need not be a Fourier transform.

We have

$$P(\zeta, \eta) = 1 \text{ over pinholes } 1 \text{ and } 2; \tag{18}$$

$$P(\zeta, \eta) = P_0 (\zeta, \eta) \text{ over the central pinhole.} \tag{19}$$

We assume that __all__ of the pinholes are small - so small that (17) is well approximated by

$$F(x,y) = A_1 \frac{e^{ikr_1}}{r_1} + A_2 \frac{e^{ikr_2}}{r_2} + \iint_{\text{over the central pinhole.}} P_0(\zeta, \eta) \frac{e^{ikr}}{r} d\zeta d\eta \tag{20}$$

We have to consider the remaining integral more carefully when $P_0(\zeta, \eta) \neq$ constant. Let

$$I_0 = \iint_{\text{over central pinhole}} P_0(\zeta, \eta) \frac{e^{ikr}}{r} d\zeta d\eta. \tag{21}$$

$P_0 (\zeta, \eta) \neq$ constant when the glass sample is striated.

From (17).

$$r = [x^2 + y^2 + D^2 + \zeta^2 + \eta^2 - 2(x\zeta + y\eta)]^{\frac{1}{2}} = R\sqrt{1 + \frac{\zeta^2 + \eta^2}{R^2} - 2\frac{(x\zeta + y\eta)}{R^2}} \; ;$$

where $R = r_0 = \sqrt{x^2 + y^2 + D^2}$. \tag{22}

19

Now in the experiments D will be so large relative to $\sqrt{\zeta^2 + \eta^2}$ and $|x\zeta + y\eta|$ that with excellent approximation (22) yields

$$r = R + \frac{\zeta^2 + \eta^2}{2R} - \frac{x\zeta + y\eta}{R} \; . \tag{23}$$

It suffices to set $r = R$ in the denominator of (21) to obtain

$$I_0 = \frac{e^{ikR}}{R} \iint_{\text{over the central pinhole}} P_0(\zeta,\eta) e^{ik\left[\frac{\zeta^2 + \eta^2}{2R} - \frac{x\zeta + y\eta}{R}\right]} d\zeta d\eta \tag{24}$$

Further simplifications of Eq. (24) are possible if we restrict D and therefore R to be greater than 50 meters, and restrict the diameter of the central pinhole to be equal or less than about 0.34 mm. Then $\sqrt{\zeta^2 + \eta^2} = 0.34/2$, hence with respect to Eq. (24), with $\lambda = 0.6328 \times 10^{-3}$ mm,

$$k \frac{\zeta^2 + \eta^2}{2R} = \pi \frac{\sqrt{\zeta^2 + \eta^2}}{\lambda} \frac{\sqrt{\zeta^2 + \eta^2}}{R} < 0.0029 \text{ radians.} \tag{25}$$

Consider next the term $k \frac{(x\zeta + y\eta)}{R}$ along the line $y = 0$. The fringe width produced by the fringes due to the two outer pinholes is given by

$$\frac{x}{R} = \frac{\lambda}{2a} \; .$$

We now restrict our field of view to points x so near the axis that, say, $\frac{x}{R} = \frac{\lambda}{2a}$. Then $k \frac{x\zeta + y\eta}{R} = \frac{kx\zeta}{R} = k\zeta \frac{\lambda}{2a} = \pi\zeta/a$. We have $a = 7$ mm and $\zeta = 0.17$ mm. Hence for points x,y near the center of the field

$$\frac{k(x\zeta + y\eta)}{R} = 0.077 \text{ radians.}$$

Under these circumstances, the exponential in Eq. (24) is substantially constant = unity so that

$$I_o = \frac{e^{ikR}}{R} \iint_{\text{over the central pinhole}} P_o(\zeta,\eta)\, d\zeta d\eta \tag{26}$$

Returning to Eq. (20), we may now set $r_1 = r_2 = R$ in the denominator and write

$$F(x,y) = \frac{e^{ikR}}{R} \left\{ A_1 e^{ik(r_1-R)} + A_2 e^{ik(r_2-R)} + B \frac{\iint P_o(\zeta,\eta)d\zeta d\eta}{B} \right\} \tag{27}$$

where B is the area of the central pinhole and $\iint P_o(\zeta,\eta)d\zeta d\eta/B$ is the _average_ value of the complex transmittance $P_o(\zeta,\eta)$ over the pinhole.

I.5   INTRODUCTION OF THE AVERAGE OPTICAL PATH

The expected glass samples produce the variation $P_o(\zeta,\eta)$ over the central pinhole. We expect that

$$P_o(\zeta,\eta) = T\, e^{i\Delta(\zeta,\eta)} \tag{28}$$

where T is the amplitude transmittance and Δ is the optical path through the striated sample of glass. T will be substantially constant but not $\Delta(\zeta,\eta)$.

Let Δ_a be the average value of the optical path over the area of the pinhole. Then

$$P_o(\zeta,\eta) = T\, e^{i\Delta_a}\, e^{i[\Delta(\zeta,\eta)-\Delta_a]} . \tag{29}$$

We assume now that $\Delta(\zeta,\eta)-\Delta_a$ is no larger but that

$$e^{i[\Delta(\zeta,\eta)-\Delta_a]} \rightarrow 1 + i\,[\Delta(\zeta,\eta)-\Delta_a] ; \tag{30}$$

21

i.e. terms $\dfrac{[\Delta(\zeta,n)-\Delta_a]^2}{2}$ and higher ordered terms are negligible. Then

$$I \equiv \iint_{\text{over central pinhole}} P_0(\zeta,\eta)\,d\zeta d\eta \qquad = T\,e^{i\Delta_a} \iint [1+i(\Delta(\zeta,\eta)-\Delta_a)]\,d\zeta d\eta$$

$$= T\,e^{i\Delta_a} \left\{ B - iB\Delta_a + i\iint \Delta(\zeta,\eta)\,d\zeta d\eta \right\}$$

$$= T\,e^{i\Delta_a} \left\{ B - iB\Delta_a + iB\Delta_a \right\}. \tag{31}$$

In summary from Eq. (31)

$$I = T\,B\,e^{i\Delta_a} = \iint_{\text{over central pinhole}} P_0(\zeta,\eta)\,d\zeta d\eta \tag{32}$$

For this to be true, the variation $\Delta(\zeta,\eta)-\Delta_a$ must be small enough that in the expansion (30) the term $\dfrac{i^2[\Delta(\zeta,\eta)-\Delta_a]^2}{2!}$ and all higher ordered terms are negligible. This offers considerable information about the allowable variation.

Finally in summary from Eqs. (?7) and (32) we obtain

$$F(x,y) = \frac{e^{ikR}}{R} \left\{ A_1 e^{ik(r_1-R)} + A_2 e^{ik(r_2-R)} + T\,B\,e^{i\Delta_a} \right\}; \tag{33}$$

A_1 = area of pinhole 1:

A_2 = area of pinhole 2:

B = area of central pinhole.

T = amplitude transmittance of the glass plate.

Δ_a = average optical path of the glass sample over the area of the central pinhole with Δ in radians.

$$R = \sqrt{x^2+y^2+D^2} \; ; \tag{33a}$$

$$r_1 = [(x-a)^2+y^2+D^2]^{\frac{1}{2}}; \quad r_2 = [(x+a)^2+y^2+D^2]^{\frac{1}{2}} \cdot \tag{33b}$$

22

Comment: When the three pinholes cannot be illuminated uniformly, one can consider A_1, A_2 and B as the product of area of the pinhole and the amplitude of the radiation thereon. It can of course happen that the phase of the radiation incident on the pinholes is not the same. For this case we can generalize Eq. (33) by writing

$$F(x,y) = \frac{e^{ikR}}{R}\left\{ A_1 e^{i\Delta_1} e^{ik(r_1 - R)} + A_2 e^{i\Delta_2} e^{ik(r_2 - R)} + T B e^{i\Delta_a} \right\} \quad (34)$$

I.6 THE FRESNEL THEORY FOR EQUALLY SPACED PINHOLES WITH $A_1 = A_2$. THE LINE $y = 0$.

Several considerations show that one should look at the fringes in the vicinity $x=y=0$. We shall take $y=0$ and x small. Then

$$R = \sqrt{x^2 + D^2} \quad (35)$$

From Eq. 33b and $y=0$

$$r_1 = \sqrt{x^2 + D^2 + a^2 - 2ax} = R\sqrt{1 + \frac{a^2}{R^2} - \frac{2ax}{R^2}} \;;$$

$$r_2 = \sqrt{x^2 + D^2 + a^2 + 2ax} = R\sqrt{1 + \frac{a^2}{R^2} + \frac{2ax}{R^2}} \cdot \quad (36)$$

We will have $1 \gg \frac{a^2}{R^2}$ or $\frac{|2ax|}{R^2}$. Then approximately

$$r_1 = R\left\{ 1 + \frac{a^2}{2R^2} - \frac{ax}{R^2} - \frac{1}{8}\left(\frac{a^2}{R^2} - \frac{2ax}{R^2} \right)^2 \right\} \;;$$

$$r_2 = R\left\{ 1 + \frac{a^2}{2R^2} + \frac{ax}{R^2} - \frac{1}{8}\left(\frac{a^2}{R^2} + \frac{2ax}{R^2} \right)^2 \right\} \cdot \quad (37)$$

23

$$r_1 - R = \frac{a^2}{2R} - \frac{ax}{R} - \frac{1}{8R^3}\left(a^4 - 4a^3x + 4a^2x^2\right) ;$$

$$r_2 - R = \frac{a^2}{2R} + \frac{ax}{R} - \frac{1}{8R^3}\left(a^4 + 4a^3x + 4a^2x^2\right) \cdot \tag{37a}$$

In order to obtain good fringes, the terms in x^2 must be negligible. This will be the case if we observe, as we should, in the vicinity of $x=y=o$. Then

$$r_1 - R = \frac{a^2}{2R}\left(1 - \frac{a^2}{4R^2}\right) - \frac{ax}{R}\left(1 - \frac{a^2}{2R^2}\right) ;$$

$$r_2 - R = \frac{a^2}{2R}\left(1 - \frac{a^2}{4R^2}\right) + \frac{ax}{R}\left(1 - \frac{a^2}{2R^2}\right) \cdot \tag{37b}$$

Let the result (37b) be entered into Eq. (34). Then

$$F(x,y) = \frac{e^{ikR}}{R}\, e^{ik\frac{a^2}{2R}\left(1-\frac{a^2}{4R^2}\right)}\, e^{i\frac{\Delta_1+\Delta_2}{2}} \left\{ A_2\, e^{i\frac{\Delta_2-\Delta_1}{2}}\, e^{i\frac{kax}{R}\left(1-\frac{a^2}{2R^2}\right)} \right.$$

$$\left. + A_1\, e^{-i\frac{\Delta_2-\Delta_1}{2}}\, e^{-i\frac{kax}{R}\left(1-\frac{a^2}{2R^2}\right)} + T B\, e^{-i\frac{\Delta_1+\Delta_2}{2}}\, e^{i\Delta_a}\, x \right.$$

$$\left. e^{-ik\frac{a^2}{2R}\left(1-\frac{a^2}{4R^2}\right)} \right\} \cdot \tag{38}$$

The irradiance $H(x,y)$ is given by

$$H(x,y) = |F(x,y)|^2 \cdot \quad \text{Hence} \tag{39}$$

$$H(x,y) = \frac{1}{R^2}\left| A_2\, e^{i\frac{\Delta_2-\Delta_1}{2}}\, e^{i\frac{kax}{R}\left(1-\frac{a^2}{2R^2}\right)} + A_1\, e^{-i\frac{\Delta_2-\Delta_1}{2}}\, e^{-i\frac{kax}{R}\left(1-\frac{a^2}{2R^2}\right)} \right.$$

$$\left. + T B\, e^{-i\frac{\Delta_1+\Delta_2}{2}}\, e^{i\Delta_a}\, e^{-ik\frac{a^2}{2R}\left(1-\frac{a^2}{4R^2}\right)} \right|^2 \tag{40}$$

Case $A_1 = A_2 = A$

$$H(x,y) = \frac{1}{R^2} \left| 2A\cos\left[\frac{kax}{R}\left(1-\frac{a^2}{2R^2}\right) + \frac{\Delta_2 - \Delta_1}{2} \right] \right.$$

$$\left. + T\,B\,e^{i\Delta_a}\,e^{-i\frac{\Delta_1+\Delta_2}{2}}\,e^{-ik\frac{a^2}{2R}\left(1-\frac{a^2}{4R^2}\right)} \right|^2 \tag{41}$$

(Like pinholes 1 and 2).

In handling and interpreting Eq. (41), it is helpful to set

$$\Phi \equiv \Delta_a - \frac{\Delta_1+\Delta_2}{2} - k\,\frac{a^2}{2R}\left(1 - \frac{a^2}{4R^2}\right). \tag{42}$$

Then

$$H(x,o) = H(x) = \frac{1}{R^2} \left| 2A\cos\left[\frac{kax}{R}\left(1-\frac{a^2}{2R^2}\right) + \frac{\Delta_2-\Delta_1}{2}\right] + T\,B\,e^{i\Phi} \right|^2$$

$$R \equiv \sqrt{x^2 + D^2} \qquad . \tag{43}$$

We remark first that sinusoidal fringes do not appear except where x is so small that with excellent approximation

$$R = D \qquad . \tag{44}$$

Of considerable practical importance, the _main_ effect of having $\Delta_2 \neq \Delta_1$ is to _shift_ the sinusoidal fringes that occur near x=y=o. This shift is of no importance to our present application of the Zernike method.

It is always possible to find a D, Fig. I-2, such that

$$\Phi = \pm\,\mu\,\frac{\pi}{2} \quad ; \quad \mu \text{ an odd integer.} \tag{45}$$

25

Then with x small

$$H(x) = \frac{1}{D^2} \; \Big|\, 2A\cos\left[\frac{kax}{D}\left(1-\frac{a^2}{2D^2}\right)\right] + T\,B\,e^{\pm i\mu\frac{\pi}{2}}\,\Big|^2 \tag{46}$$

whence

$$H(x) = \frac{1}{D^2}\left\{\, 4A^2\cos^2\left[\frac{kax}{D}\left(1-\frac{a^2}{2D^2}\right)\right] + T^2\,B^2\,\right\}; \tag{47}$$

$$\pm\,\mu\,\frac{\pi}{2} = \Delta_a - \frac{\Delta_1+\Delta_2}{2} - k\,\frac{a^2}{2D}\left(1-\frac{a^2}{4D^2}\right); \quad \mu \text{ odd}. \tag{48}$$

I.7   ON THE USE OF A COLLIMATOR AND TELESCOPE

The arrangement of Fig. I-2 is hardly practical; so we utilize the configuration of Fig. I-3.
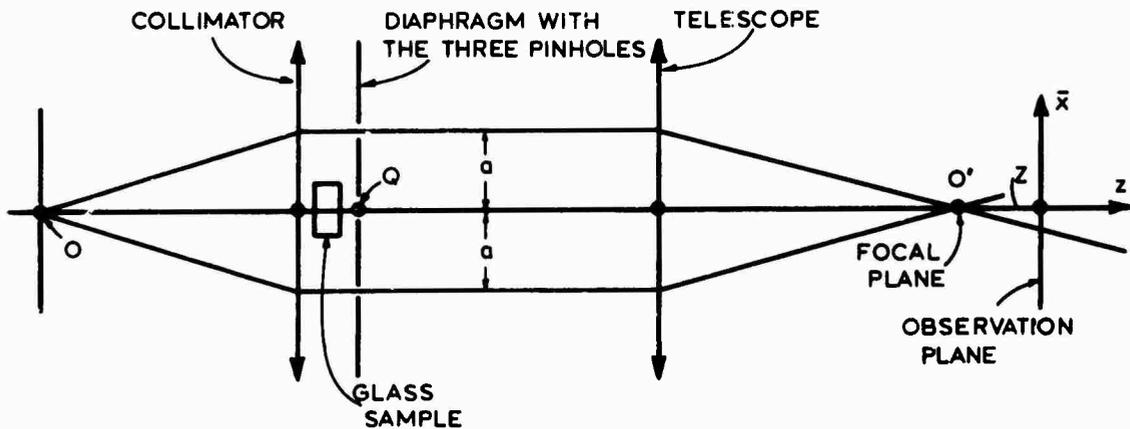
Figure I-3. The preferred optical system. Light from a laser is focused upon a small pinhole at o. The observation plane is at the distance z from the focal plane o′ of the telescope. We observe this observation plane by a 100× microscope.

26

Not all positions Q of the diaphragm are equally desirable
With Van Heel, Physica XXIV, Zernike issue, 529-531 (1958), we
prefer (as will now be explained) to locate Q at or near the
first focal plane of the telescope. We assume that both colli-
mator and telescope are highly corrected.

The problem is now to associate the out-of-focus distance
z with the distance D of Fig. I-2. We wish also to relate $\bar{x}$ in
Fig. I-3 to x of Fig. I-2. Fig. I-4 is used for this purpose.
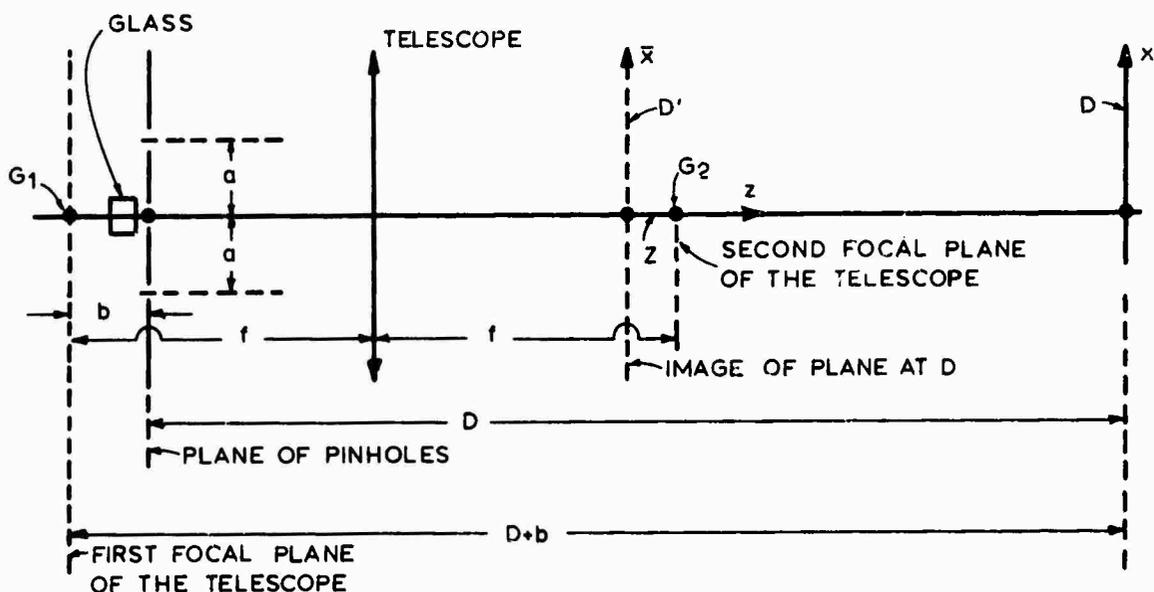
Figure I-4. Convention with respect to the image D′ of the
plane D of Fig. I-2.

Beginning with Fig. I-2, we obtain the solutions (41),
(40) or (46) for the disturbance in the plane D at distance D
from the pinholes where D falls in the far-Fresnel region.
This is to say that in the absence of the telescope we know the
solution in plane D, Fig. I-4. When the telescope is inserted,
plane D is imaged at a plane D′ such that in accordance with
Newton's formula

$$f^2 = -(D+b)z \tag{44}$$

where the plane of the three pinholes falls at distance b to
the right of the 1st focal plane of the telescope. In this

27

Newton's for .ula (D+b) and z are the object and image distance, respectively, from the focal points G_1 and G_2. From Eq. (49)

$$D = -\left(\frac{f^2}{z} + b\right) \text{ or } \frac{1}{D} = -\frac{z}{f^2+bz} \; . \tag{50}$$

We may think of distance z as the out-of-focus distance.

Let us apply (50) to the result (47). Then

$$H(x) = \frac{1}{D^2}\left\{ 4A^2 \cos^2\left[\frac{kax}{D}\left(1-\frac{a^2}{2D^2}\right)\right] + T^2 B^2 \right\} \text{ , with} \tag{51}$$

D given by Eq. (50). Now in (48), the glass plate is so thick that μ is going to be some large, positive, odd number. Thus we choose the + sign and write

$$\Delta_a = \mu\,\frac{\pi}{2} + \frac{\Delta_1+\Delta_2}{2} - \frac{ka^2}{2}\,\frac{z}{f^2+bz}\left(1 - \frac{a^2}{4}\,\frac{z^3}{(f^2+bz)^3}\right) \; . \tag{52}$$

At this point, we neglect $a^2/2D^2$ as compared to unity and $\frac{a^2}{4}\,\frac{z^3}{(f^2+bz)^3}$ as compared to unity. This does mean that we should be looking in the region where z is small, that is, near focus. Eqs. (51) and (52) now assume their practical form

$$H(x) = \frac{1}{D^2}\left[4A^2 \cos^2\left(\frac{kax}{D}\right) + T^2 B^2 \right] \; ; \tag{53}$$

$$\Delta_a = \mu\,\frac{\pi}{2} + \frac{\Delta_1+\Delta_2}{2} - \frac{ka^2 z}{2(f^2+bz)} \; . \tag{54}$$

As pointed out by Van Heel, we now see that Δ_a is linear in the out-of-focus distance z, Fig. I-4, when b=o, i.e. when the plane of the pinholes is located at the 1st focal plane of the telescope. Our experiments have confirmed this conclusion.

28

To summarize matters up to this point, we choose $\Phi = \mu \frac{\pi}{2}$ where Φ is given by Eq. (42). Then the irradiance $H(x)$ is given by Eq. (53) provided the two outer pinholes have equal area and are equally illuminated. The fringe settings for Eq. (53) are sharp, i.e. the values of z at which the fringes assume this doubled appearance are sharp. The values of z at which $\Phi = o, \pm \pi, \pm 2\pi$, etc. are not sharp and are not a good measure of Δ_a. We utilize Eq. (54) as follows. With an initial pressure on the glass sample, Fig. I-3, and for the assigned direction of vibration of the electric vector

$$\left(\Delta_a\right)_o = \mu \frac{\pi}{2} + \frac{\Delta_1 + \Delta_2}{2} - \frac{k\ a^2\ z_o}{2(f^2 + bz_o)} \cdot \tag{55a}$$

For the pressure P_1

$$\left(\Delta_a\right)_1 = \mu \frac{\pi}{2} + \frac{\Delta_1 + \Delta_2}{2} - \frac{k\ a^2\ z_1}{2(f^2 + bz_1)} ; \tag{55b}$$

since we alter z so as to keep the order number μ the same and since neither Δ_1 nor Δ_2 are altered. Thus

$$\left(\Delta_a\right)_1 - \left(\Delta_a\right)_o = -\frac{ka^2}{2}\left[\frac{z_1}{f^2 + bz_1} - \frac{z_o}{f^2 + bz_o}\right] \cdot \tag{55c}$$

Then with b=o or negligible

$$\left(\Delta_a\right)_1 - \left(\Delta_a\right)_o = -\frac{ka^2}{2f^2}(z_1 - z_o) = \frac{\pi}{\lambda}\frac{a^2}{f^2}(z_o - z_1) . \tag{55d}$$

In case $\left(\Delta_a\right)_1 > \left(\Delta_a\right)_o$, $z_o > z_1$, $\tag{55e}$

a fact which we confirm experimentally.

We seek next to introduce the actual coordinate $\bar{x}$ of the plane of observation D' of Fig. I-4. To do this, we use the simplified Fig. I-5. This indicates the first order optics that become involved.
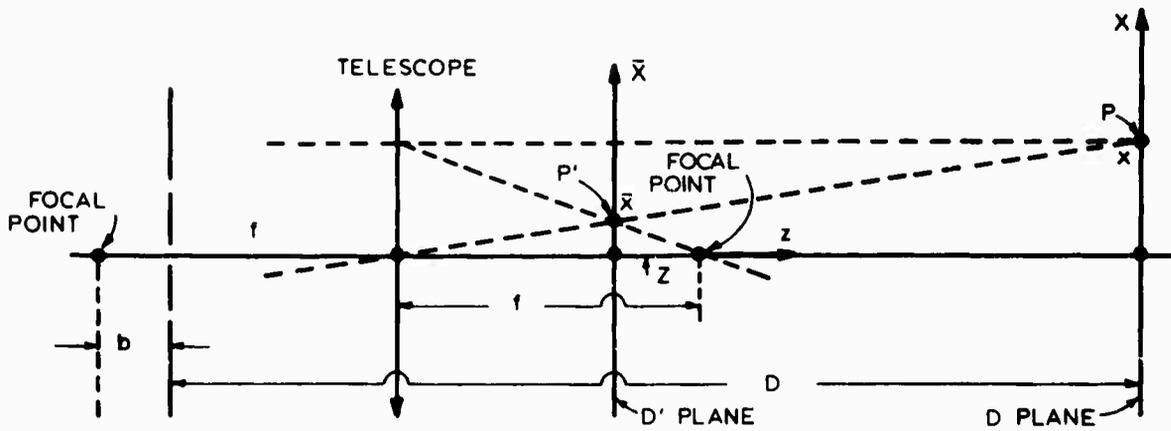
Figure I-5. Illustrating the first order connection between $\bar{x}$ and x.

From Fig. I-5, if $|M|$ = magnification

$$|M| = \frac{f+z}{D-(f-b)} = \frac{f+z}{D-f+b} = \frac{\bar{x}}{x} \qquad (56)$$

where $z < o$ in the figure. We should have

$$M = \frac{- (\text{image distance})}{f} = \frac{-z}{f} . \qquad (57a)$$

Let us check this matter. From Eqs. (50) and (56)

$$M = \frac{f+z}{-\frac{f^2+zb}{z} -f+b} = \frac{(f+z)z}{-f^2-zb+zb-zf} = \frac{z(f+z)}{-f(f+z)} = -\frac{z}{f} . \qquad (57b)$$

$$\therefore \quad x = \frac{\bar{x}}{M} = -\frac{\bar{x}f}{z} . \qquad (58)$$

With reference to Eq. (53)

$$\frac{ax}{D} = -\frac{a}{D}\frac{\bar{x}f}{z} = -\frac{a\bar{x}f}{z}\frac{(-z)}{f^2+bz} = \frac{af\bar{x}}{f^2+bz} . \qquad (59)$$

30

$$H(\bar{x}) = \frac{1}{D^2} \left\{ 4A^2 \cos\left(\frac{ka\bar{x}}{f+\frac{b}{f}z}\right) + T^2 B^2 \right\} . \tag{60}$$

At b=o, not only is Φ or Δ_a linear in the out-of-focus distance z but also the fringe width for fields near x=y=o is constant. We have from (60)

$$H(\bar{x}) = \frac{1}{D^2} \left\{ 4A^2 \cos^2\left(\frac{ka\bar{x}}{f}\right) + T^2 B^2 \right\} \text{ or}, \tag{61}$$

more conveniently, since the external factor is unimportant

$$H(\bar{x}) = 4A^2 \cos^2\left(\frac{ka\bar{x}}{f}\right) + T^2 B^2 , \tag{61a}$$

holding for outer pinholes having the same area.

Also from Eq. (42) for Φ with R→D and $\frac{1}{D} = \frac{-z}{f^2}$ with $a^2/4R^2$ negligible

$$\Phi = \Delta_a + \frac{\Delta_1 + \Delta_2}{2} + \frac{ka^2}{2f^2} z = \Delta_a + \frac{\Delta_1 + \Delta_2}{2} + \frac{\pi}{\lambda} \frac{a^2}{f^2} z . \tag{62}$$

where Δ_a, Δ_1 and Δ_2 are to appear in radians. For highly cor-rected telescopes and well centered systems we may take

$$\Delta_1 = \Delta_2 = o . \tag{62a}$$

At our settings that produce the distribution (61), we set z so that $\Phi = \mu \frac{\pi}{2}$, μ odd.

31

I.8 TOLERANCE ON THE TILT OF THE SAMPLE

The most damaging effect of the tilt of the sample from perpendicularity to the incident beam is the change in tilt that may be produced upon changing the applied pressure. The following considerations are based upon Fig. I-6 and apply to a single passage of light through the sample.

Let the normal to the sample be tilted by the amount θ from the axis A B of the instrument. Then with respect to Fig. I-6

$$\ell = \frac{L}{\cos\phi} \; ; \quad z = \ell \; \cos(\theta-\phi) = L \; \frac{\cos(\theta-\phi)}{\cos\phi} \tag{63}$$
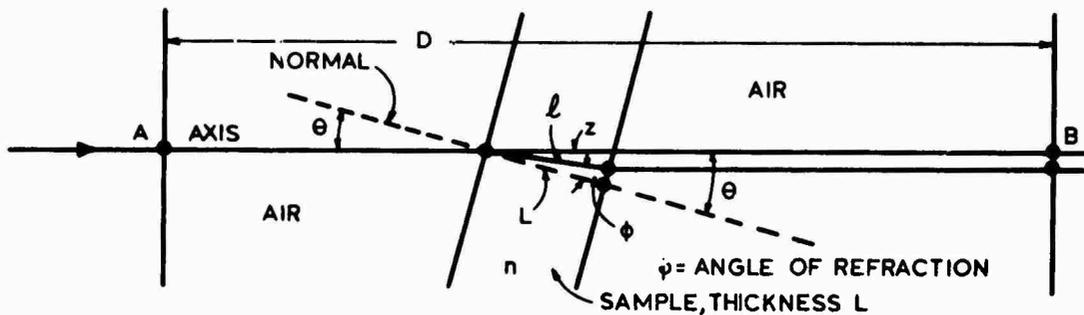
Figure I-6. Convention with respect to tilt of the sample.

Let

$$\Delta = \text{optical path from A to B} = D - z + n\ell.$$

$$\therefore \quad \Delta = D - L \; \frac{\cos(\theta-\phi)}{\cos\phi} - \frac{nL}{\cos\phi} \; . \tag{64}$$

Let $\Delta_0 = \Delta_{\theta=0} = D - L + nL.$ $\tag{65}$

Define

$$\delta = \Delta - \Delta_0 = \text{change in optical path due to tilt.} \qquad (66)$$

One finds quite directly from (64) - (66) that

$$\delta = L \left[\frac{n(1-\cos\phi)}{\cos\phi} + \frac{\cos\phi - \cos(\theta-\phi)}{\cos\phi} \right] \quad \text{or}$$

$$\frac{\delta}{L} = 1 + \frac{n(1-\cos\phi)}{\cos\phi} - \frac{\cos(\theta-\phi)}{\cos\phi} \quad ; \quad \sin\theta = n \sin\phi \quad ; \quad \text{any } \theta. \qquad (67)$$

For $\underline{\text{small}}$ θ, write $\cos\phi = 1 - \frac{\phi^2}{2}$; $\theta = n\phi$. Then

$$\frac{\delta}{L} = \frac{\theta^2}{2} \frac{n-1}{n} \quad \text{and} \quad \theta = \sqrt{\frac{2n}{n-1} \frac{\delta}{L}} \quad . \qquad (68)$$

Hence for small tilts about the normal position the optical path error δ varies as θ^2.

TABLE I.1 TOLERANCES θ AS COMPUTED FROM EQ. (68)

Error δ	n	L (mm)	θ (min)	λ (μm)
$\lambda/1000$	1.5	10	1.88	0.5
$\lambda/1000$	1.5	10	2.12	0.6328
$\lambda/100$	1.5	10	6.70	0.6328
$\lambda/100$	1.6	10	3.55	0.6328

It appears from this table that the tolerances on tilt are quite liberal; but such is not the case when the sample is not normal to the incident beam $\underline{\text{before}}$ the added tilt occurs. For example, if the sample has originally the tilt $\theta_0 = 0.1°$, then if this tilt is altered to $0.15°$ by changing the pressure, δ/λ changes from 0.00802 to 0.01803 due to change of tilt alone.

33

This means that a change of tilt of 3 minutes causes an error in δ of 0.01 wavelength - an amount large enough to interfere with the accuracy of our measurements. If $\theta_0 = 0.1°$, the added tilt should be constrained to about one minute.

Eq. (68) is accurate enough for $o \lesssim \theta \lesssim 2°$, a range which, surely, should not be exceeded for experimental reasons. From Eq. (68)

$$\frac{\delta_1 - \delta_0}{\lambda} = \frac{L}{\lambda} \frac{n-1}{2n} (\theta_1^2 - \theta_0^2) . \tag{69}$$

A definite tolerance on θ_1 cannot be assigned without knowing θ_0. Since it is desirable to measure the optical path differences to 0.01λ, it is suggested that θ_1 be restricted with respect to θ_0 such that

$$\frac{L}{\lambda} \frac{n-1}{2n} (\theta_1^2 - \theta_0^2) \lesssim 2 \times 10^{-3} \tag{70}$$

In conclusion, it is suggested that the head of a collimating device be placed just beyond the pinhole O, Fig. I-3 for measuring how nearly normal the surfaces of the glass sample are to the incident beam. Means for adjustment should be provided so that Eq. (70) remains satisfied. Motion of the cross-hairs in two, perpendicular directions is indicated.